Lithium-Sulfur Cell State of Charge Estimation Using a Classification Technique

Neda Shateri, Zhihao Shi, Daniel J. Auger, *Senior Member, IEEE*, and Abbas Fotouhi, *Member, IEEE*

***Abstract*—Lithium-Sulfur (Li-S) batteries are a promising next-generation technology providing high gravimetric energy density compared to existing lithium-ion (Li-ion) technologies in the market. The literature shows that in Li-S, estimation of state of charge (SoC) is a demanding task, in particular due to a large flat section in the voltage-SoC curve. This study proposes a new SoC estimator using an online parameter identification method in conjunction with a classification technique. This study investigates a new prototype Li-S cell. Experimental characterization tests are conducted under various conditions; the duty cycle – intended to represent a real-world application – is based on an electric city bus. The characterization results are then used to parameterize an equivalent-circuit-network (ECN) model, which is then used to relate real-time parameter estimates derived using a Recursive Least Squares (RLS) algorithm to state of charge using a Support Vector Machine (SVM) classifier to estimate an approximate SoC range. The estimate is used together with a conventional coulomb-counting technique to achieve continuous SoC estimation in real-time. It is shown that this method can provide an acceptable level of accuracy with less than 3% error under realistic driving conditions.**

***Index Terms*—Lithium-sulfur battery, parameter identification, state of charge estimation, SVM classifier.**

I. Introduction

BATTERY technology is vital for electric vehicles, and for full parity with internal combustion engines, it is essential to develop technologies that will decrease battery cost, decrease the charging time and increase the range of EVs. There are various strands of research, and one promising technology is the lithium-sulfur (Li-S) battery. Compared to existing Li-ion technologies, Li-S batteries can potentially provide higher specific energy, improved safety, and – when productionized – a lower unit cost due to the wide availability of sulfur and the lack of dependence on scarce heavy metals. There are limitations to be overcome such as poor instantaneous power capabilities, high self-discharge and short cycle life [1]. These would need resolution for most mainstream automotive applications and are the subject of ongoing electrochemical research [2]. In parallel with the efforts which are going on by electrochemists to build new Li-S cells with superior features, control engineers are also trying to understand particular challenges associated with the management of Li-S battery technologies to support specialist niche vehicle applications and so that as electrochemical advances are made, it is possible to take advantage of them in more mainstream electric vehicles. Battery management for Li-S is not directly comparable to that of most Li-ion cells, mainly due to the Li-S cell's flat voltage curve versus state-of-charge (SOC) [3]. This study is focused on development of a new SoC estimation technique for Li-S battery to be used in an EV, making use of state-of-the art algorithmic techniques that have not been applied to Li-S before.

Various battery SoC estimation approaches are described in the literature [4]–[7]. A good summary of such techniques is presented in [8] and [9]. One of the well-known methods of battery SOC estimation is called 'coulomb-counting' that works based on integration of the load current over time. Although coulomb-counting method is useful in theory, it is not a stand-alone method in practice. This method requires a good estimate of the initial SOC and the battery capacity (C_t) which are not always available [10], [11]. In addition, coulomb-counting suffers from accumulated measurement errors and it is can drift away from the correct value of SoC [12], [13]. Other techniques for battery SoC estimation are look-up tables that relate battery SoC to its open-circuit-voltage (OCV) curve, and also proportional-integral (PI) observer method that works based on a linearized model of the cell [14]. Although, these methods have been used widely for Li-ion batteries, it is not applicable for a Li-S cell because of the flat shape of the OCV-SoC curve of Li-S as explained in [15]. Recursive adaptive filters are another group of SoC estimation algorithms in the literature which have been used for automotive application [16]–[19]. Good examples of such estimators are Kalman filter derivatives and particle filter estimators [20]–[25]. In addition to these SoC estimation techniques (which rely solely on models that are characterized as a priority), another group of estimators work based on online battery model identification. In these techniques, a model (often an equivalent-circuit model) is fitted to battery measurement data in real-time and then the model's parameters are used for battery state estimation [26]–[28]. Although there are a number of studies in the literature in which Li-ion battery models are used beside a SoC estimator, few similar studies exist for Li-S battery. Looking at the literature, a first version of Kalman filter-based SoC estimators have been recently developed for Li-S cells in [29]–[31]. An alternative body of work has used Adaptive

Manuscript received March 24, 2020; revised July 22, 2020 and September 20, 2020; accepted November 15, 2020. Date of publication December 16, 2020; date of current version February 12, 2021. This work was supported by the European Commission under Grant Agreement 814471 and Innovate UK under Grant TS/R013780/1. The review of this article was coordinated by Prof. X. Hu. *(Corresponding author: Daniel J. Auger.)*

The authors are with the Advanced Vehicle Engineering Centre, Cranfield University, MK43 0AL Bedfordshire, U.K. (e-mail: shaterineda@gmail.com; v.shi@cranfield.ac.uk; d.j.auger@cranfield.ac.uk; abfotouhi@gmail.com).

Digital Object Identifier 10.1109/TVT.2020.3045213

Neuro-Fuzzy Inference Systems (ANFIS) [3]. Although both techniques have been successfully applied for Li-S cell SoC estimation, there are other techniques that may be more effective, particularly as the field matures into applications with duty-cycle aged cells, and it is valuable to understand other techniques that can be applied. This paper describes a new approach, based on classification via a Support Vector Machine.

The new technique includes two stages: a real-time parameter identifier using a Recursive Least Squares (RLS) algorithm, and the state estimator itself which uses the identified parameters as inputs to a Support Vector Machine (SVM) which estimates battery state. This method is a combination of 'system identification' and 'classification' techniques. The results are also combined with coulomb counting, to give continuous estimates. The RLS algorithm is used for cell model identification as a quick online technique which has been widely used in the literature [32], [33]. In the RLS method, the model's error (i.e., a function of the model's parameters) is minimized using an iterative procedure [34]. SVM methods have also been widely used in the literature for modelling, prediction and classification in different applications since 1998 in a variety of engineering areas [35], [36]. SVM methods have been used for SoC estimation in other battery types, such as lithium-ion-polymer (LiP) [37], nickel metal hydride NiMH [38], lithium iron phosphate (LiFePO4) cell [39], [40] and lithium iron manganese phosphate (LiFeMnPO4) [41]. In [42] and [43], also an optimized Support Vector Regression (SVR) model is used to develop a battery SoC estimator for EV application. Their results have then been compared favorably with those obtained from an Artificial Neural Network (ANN). In those studies, different inputs to the SVM have been considered such as current–voltage–temperature and current–voltage–required-power as the inputs of SVM. These studies suggest that SVM technique can outperform ANNs and this is one of the reasons that SVM is chosen and investigated in this study.

Since the proposed SVM SoC classifier only generates a discrete cluster number (between 1 and 10 in this case), it cannot by itself provide a smooth continuous SoC estimate. In order to have a continuous SoC estimation in real-time, the proposed model-based classifier is combined with a coulomb-counting technique. Using such a hybrid system, not only a continuous SoC estimation is achieved but also the accuracy is improved. To test the effectiveness, the results are compared with an after-the-event coulomb counting.

Structure of this article is as follows: in Section II, specifications, characterization test and modelling approach of the Li-S cell is explained. Section III then contains Li-S cell SoC classification using SVM based on the identification results. Finally, combination of coulomb-counting and the proposed model-based SoC classifier is explained and the results are evaluated in Section IV.

II. Li-S Cell: Specifications, Characterization Test, and Modelling

A. Li-S Cell Specifications

The lithium-sulfur cell that is considered in this study is supplied by OXIS Energy Ltd [44] with the specifications listed in Table I. It should be noted that the cell is a prototype with energy density of 290 Wh/kg however, the final product is expected to have an energy density more than 400 Wh/kg [44].

TABLE I
Specifications of the Prototype Li-S Cell

Parameter	Value
Capacity	19 (Ah)
Nominal voltage	2.15 (V)
Cell mass	141 (g)
Maximum voltage	2.6 (V)
Minimum voltage	1.9 (V)
Maximum discharge rate	3C ~ 57 (A)
Maximum charge rate	0.25C ~ 4.75 (A)

B. Li-S Cell Characterization Test

The Li-S cell test equipment is shown in Fig. 1. The test rig includes a power source/sink that applies a desirable current profile to the cell and measures its terminal voltage, and a thermal chamber to control the temperature during the test. Two types of test have been conducted: (i) pulse test, and (ii) drive cycle test. In both cases, a current profile is programmed to be applied to the cell and the cell's terminal voltage is measured as the output. All tests are started from fully charged state (2.6 V) and are continued until fully-discharged state (based on cut-off voltage of 1.9 V). Accordingly, cell parametrization is possible at different SoC levels. Data is collected in the time domain with a sampling rate of 1 Hz including time, temperature, current and terminal voltage. The reason of choosing a relatively low sampling rate is that an estimator that is designed to work with 1 Hz sampling rate (i.e., the worst-case scenario), also works with 10 Hz or higher sampling rates.

In the pulse test, consecutive current pulses are applied to the cell with a 'relaxation time' in between. Pulse tests are very common for cell characterization since the cell model's parameters can be observed better comparing to a random current profile. On the other hand, in the drive cycle test, a more realistic dynamic current profile is used based on a standard automotive drive cycle. For this purpose, the EV power demand on the Millbrook London Transport Bus (MLTB) drive cycle [45], [46] is scaled and applied to a single cell. Both pulse and MLTB test results are shown in Fig. 2. Similar to the pulse test where the current pulse is repeated until battery depletes, the MLTB current profile is repeated in the MLTB test until depletion of the cell. To have a clearer view about this, Fig. 2 also presents a zoomed window including only one MLTB cycle. One difference between the MLTB and pulse tests is that the MLTB test also includes short charging in between (negative current in the figure) as well. This is designed to simulate regenerative braking in such an application. Generally speaking, pulse tests are useful for model development and drive cycle tests are more suitable for model validation.

(a) (b) (c)

Fig. 1. Cell test equipment: (a) thermal chamber, (b) power source-sink, (c) Li-S cell.

The idea behind choosing the electric city bus application for Li-S cell is its unique advantage (i.e., higher specific energy) that enables us to store more energy on board to increase the EV range. An electric city bus is expected to operate during the day (around 16 hours) and be charged slowly over night in depot. Comparing to other drive cycles, MLTB contains lots of idle time and also low speed movement that causes less energy consumption per cycle. That means lower maximum power demand and consequently lower discharge rate, which is ideal for Li-S cell technology.

C. Li-S Cell Modelling Approach

An equivalent-circuit-network (ECN) model is parameterized using the data obtained from the Li-S cell's characterization tests. ECN modelling approach is chosen because of its effectiveness in both accuracy and computational speed [47]–[49]. A review on different battery modelling approaches is presented in [47]. In this study, an ECN model, called 'Thevenin model' [50], is used as illustrated in Fig. 3. It consists of a voltage source U_{OC}, representing the open circuit voltage of the battery, and three physical components: (i) ohmic resistor R_O that corresponds to the heating losses, (ii) polarization resistor R_P and (iii) polarization capacitor C_P. According to the Thevenin model, dynamic behavior of the battery can be described as follows:

$$\frac{dU_p}{dt} = -\frac{1}{R_pC_p}U_p + \frac{1}{C_p}I_L \tag{1}$$

$$U_L = U_{oc} - U_p - R_0I_L \tag{2}$$

Where U_p is the voltage across the polarization capacitor, and U_L and I_L are the terminal voltage and load current respectively.

(2) can be written in frequency domain using Laplace transformation:

$$s \cdot U_p\ (s) = -\frac{1}{R_pC_p} \cdot U_p\,(s) + \frac{1}{C_p}I_L\,(s) \tag{3}$$

Consequently, U_p can be expressed as:

$$U_p\ (s) = \frac{\frac{1}{C_p}I_L\,(s)}{s + \frac{1}{R_pC_p}} \tag{4}$$

Substituting U_p from (4) into (2), terminal voltage in frequency domain is:

$$U_L\,(s) = U_{oc} - \frac{\frac{1}{C_p}I_L\,(s)}{s + \frac{1}{R_pC_p}} - R_0I_L\,(s) \tag{5}$$

To transfer it from continuous-time to discrete-time domain, the bilinear transform $s = \frac{2}{T}\frac{z-1}{z+1}$ is applied to the above equation:

$$\frac{U_L\,(z) - U_{oc}}{I_L\,(z)} = \frac{-(TR_p+TR_0+2R_0R_pC_p)-(TR_p+TR_0-2R_0R_pC_p)z^{-1}}{T+2R_pC_p+(T-2R_pC_p)z^{-1}} \tag{6}$$

As a result, the terminal voltage at moment k, can be obtained from the current signal value at moment k and the terminal voltage and current signals at previous moment k-1 as follows:

$$U_L\,(k) = \theta_1 \cdot U_L\,(k-1) + \theta_2 \cdot I_L\,(k) + \theta_3 \cdot I_L\,(k-1) + \theta_4 \tag{7}$$

Where the parameters $\theta_1, \theta_2, \theta_3$ and θ_4 are defined as follows:

$$\theta_1 = \frac{2R_pC_p - T}{T + 2R_pC_p} \tag{8}$$

$$\theta_2 = -\frac{TR_p + TR_0 + 2R_0R_pC_p}{T + 2R_pC_p} \tag{9}$$

$$\theta_3 = -\frac{TR_p + TR_0 - 2R_0R_pC_p}{T + 2R_pC_p} \tag{10}$$

$$\theta_4 = \frac{2T}{T + 2R_pC_p}\,U_{oc} \tag{11}$$

(7) can be written in a more standard form for the later use of identification:

$$U_L\ (k) = \varphi^T \cdot \theta \tag{12}$$

where $\varphi = [U_L(k-1); I_L(k); I_L(k-1); 1]$ and $\theta = [\theta_1; \theta_2; \theta_3; \theta_4]$.

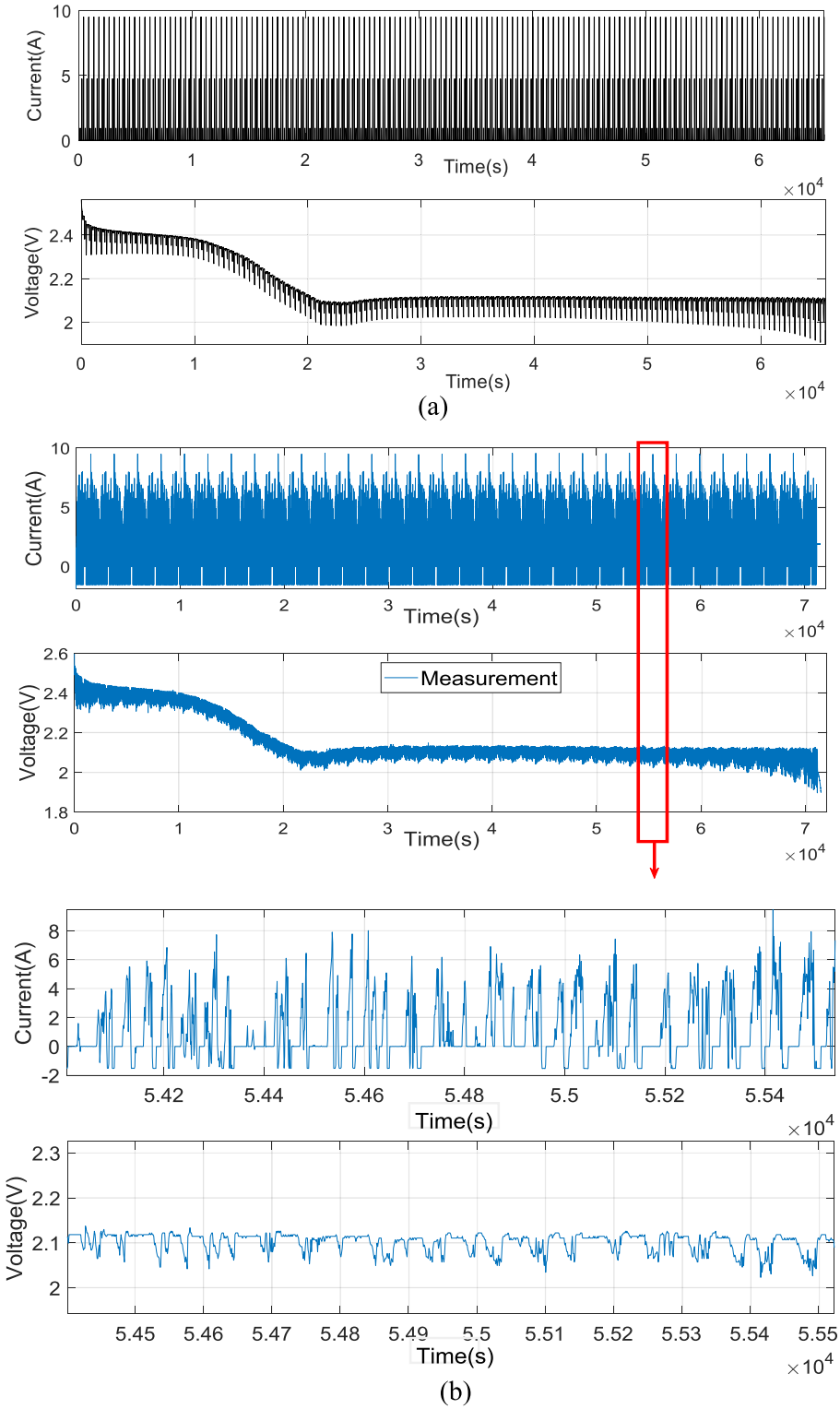

Fig. 2. Li-S cell test measurements: (a) pulse test, (b) MLTB test.

D. Li-S Cell Model Parameterization Using Forgetting Factor Recursive Least Square (FFRLS) Algorithm

Because of the application of this study in EVs, it is desirable to have a simple and quick algorithm suitable for real-time application. For this reason, Forgetting Factor Recursive Least Square (FFRLS) identification algorithm [33] is used in this study to identify parameters of the discrete model presented in (12). The model has four unknown parameters to be identified: R_0, R_p, C_p and U_{oc} which are formulated in the parameters vector θ. According to the FFRLS algorithm, the parameters

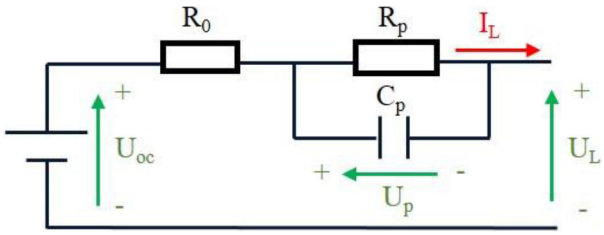

Fig. 3. Thevenin battery model.

vector is updated at each iteration as follows:

$$\hat{\theta}\ (k) = \hat{\theta}\ (k-1) + K\,(k) \cdot \left[U_L\,(k) - \varphi^T \cdot \hat{\theta}\,(k-1)\right] \quad (13)$$

Where K is the correction gain obtained from:

$$K\ (k) = P\,(k-1) \cdot \varphi \cdot \left[\gamma + \varphi^T \cdot P\,(k-1) \cdot \varphi\right]^{-1} \quad (14)$$

$$P\ (k) = \frac{1}{\gamma}\left[I - K\,(k) \cdot \varphi^T\right] \cdot P\,(k-1) \quad (15)$$

Where P is the covariance matrix and γ is the forgetting factor, indicating the effect of historical data on identification. The forgetting factor that is obtained in this study to achieve the best identification results is 0.996.

Once $\theta_1 \sim \theta_4$ are estimated using the above equations, the original four physical parameters of the Thevenin model (R_0 , R_p, C_p and U_{oc}) can be calculated from θ as follows:

$$R_0 = \frac{\theta_3 - \theta_2}{1 + \theta_1} \quad (16)$$

$$R_p = -2\frac{\theta_1\theta_2 + \theta_3}{1 - {\theta_1}^2} \quad (17)$$

$$C_p = \frac{T(1+\theta_1)^2}{-4\,(\theta_1\theta_2 + \theta_3)} \quad (18)$$

$$U_{oc} = \frac{\theta_4}{1 - \theta_1} \quad (19)$$

The FFRLS identification algorithm is applied to the Li-S cell test data (presented in Section 2.2) to parameterize the Thevenin model as shown in Fig. 4. For model validation, the terminal voltage, U_L, is compared between the measured value and the value obtained from the proposed model as illustrated in Fig. 5. The results demonstrate that the voltage estimations at different SoC levels are very close to the measurements that proves the cell model's accuracy.

III. Li-S Cell State-of-Charge (SoC) Classification

A. SoC Classification Concept

As discussed earlier, estimation of SoC of a Li-S cell is more challenging than the other types of battery mainly because of its flat voltage curve at low plateau. Consequently, most of the existing SoC estimation techniques in the literature are not applicable for Li-S battery [15]. To tackle this issue, a new framework is used here based on online model parameterization and SoC classification as presented in Fig. 6. As mentioned before, FFRLS method is used for identification whereas the

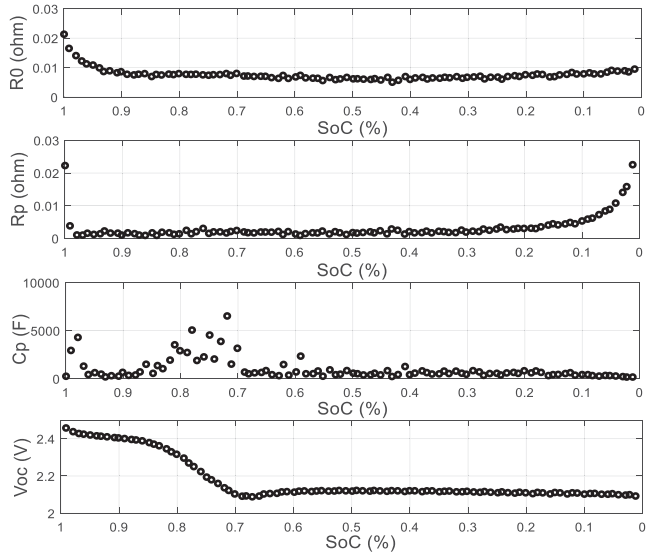

Fig. 4. Li-S cell model's parameters identified using FFRLS algorithm.

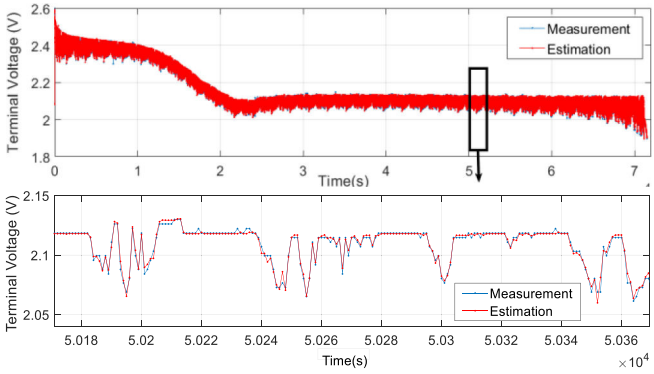

Fig. 5. Terminal voltage validation of Li-S cell model.

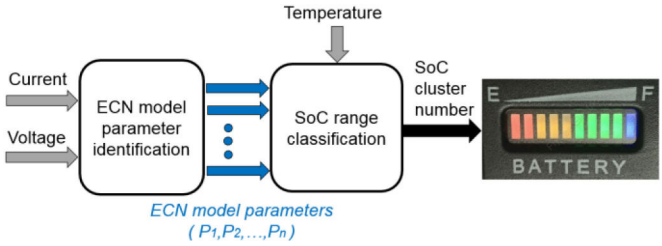

Fig. 6. Battery measurement, identification and SOC estimation.

SVM technique is used as the classifier. The theory of the SVM as type of a supervised machine learning method, which is explained in [51]. According to the literature, SVM is a quick method that is suitable for online applications.

In the proposed framework shown in Fig. 6, the identification results are served by the SVM classifier to estimate the range of SoC in form of a label between 1 and 10 (i.e., cluster number). Cluster 1 is defined to include SoC range of 0%–10%, cluster 2 for 10%–20% SoC and so on. As shown in Fig. 6, different sets of input parameters can be used for SoC classification. In this study, different combination of inputs have been tried and the results are compared as presented in Table II. To train the classifier in

TABLE II
SOC CLASSIFICATION RESULTS USING SVM AND DIFFERENT INPUTS

	Input parameters used for SoC classification					
	V_{oc}/R_o	V_{oc}/R_p	V_{oc}/C_p	$V_{oc}/R_o/R_p$	$V_{oc}/R_o/C_p$	$V_{oc}/R_o/R_p/C_p$
Training accuracy	76%	78%	68%	87%	79%	90%
Testing accuracy (hard clustering)	58%	70%	66%	67%	61%	73%
Testing accuracy (soft clustering)	79%	91%	90%	89%	80%	93%

each case, the MLTB test data is used. Each test is divided into 100 segments based on the time and then the ECN model is parameterized for each segment separately. Consequently, 100 data points are available from each test. So the inputs of the classifier are the ECN parameters and the output is SoC cluster number. In order to calculate the 'true label' (i.e., the output) for each data point, coulomb-counting method is utilized for off-line training of the classifier. Each battery experiment is repeated at least two times in order to obtain enough data for training and testing of the classifier. The structure of training and testing data is similar (in terms of inputs-output) however, the data points which are used for training, are not used again for testing.

B. Classification Results

In this Section, the results of applying the proposed SoC classifier to the Li-S cell is presented in form of classification accuracy percentage and 'confusion matrices'. Table II includes training and testing accuracy values using SVM classifier for a MLTB test at 25 °C. Different combination of inputs are considered in this study to find the best configuration that gives the highest accuracy. For both the training and testing data sets, the accuracy is defined as the ratio of the number of correctly classified data segments (each test consists of 100 segments) over the whole number of segments:

$$\text{Accuracy } (\%) = \frac{N_{\text{correct}}}{N_{\text{total}}} \times 100 \tag{20}$$

Two types of accuracy measures are calculated called 'hard clustering' and 'soft clustering'. In 'hard clustering', a segment is considered as a correctly classified one (counted for N_{correct}) when the estimated cluster number is exactly same as the expected 'true cluster number'. On the other hand, in 'soft clustering', allocation of a data segment to the neighbor cluster is also acceptable. That means for example, if the true cluster number is 3, all estimations of 2, 3 and 4 are counted for N_{correct} but not an output of 1, 5, 6, etc. The results presented in Table II show that using all four parameters of the Thevenin model (R_0, R_p, C_p and U_{oc}) gives slightly higher level of accuracy.

In addition to the numerical results presented in Table II, the confusion matrix of each classifier is presented in Fig. 8 in form of colorful graphical pictures showing the levels of uncertainty at different SoC levels. In each matrix, the rows present the true cluster number whereas the columns present the estimated cluster number. The green cells contain percentage of correct classifications while the red cells represent percentage of incorrect allocations. For example, Fig. 8(a) presents performance of the classifier using two inputs, V_{oc} and R_o. In that case, true and estimated cluster numbers are matched 100% for cluster number 10 (the bottom row) which corresponds to the SoC range between 90% to 100%. This result is in accordance to our expectation since SoC estimation is easier at high plateau where voltage curve has a clear gradient. Again from Fig. 8(a), it is clear that cluster number 6 has the worst accuracy that is around 10%. This result also looks quite reasonable because the most challenging region of Li-S SoC estimation is in the middle when the voltage curve is completely flat. As explained earlier, the red cells show the percentage of inaccurate predictions. For example, in the first row (cluster 1), 78% of the data points are classified correctly while 22% of them are classified incorrectly into cluster number 2.

Fig. 7. Thermal camera used for checking cell's surface temperature during the tests.

Similarly, the confusion matrix presented in Fig. 8(b) indicates 100% precision in prediction of cluster 1 and 10 that means high accuracy at very high and very low SoC levels. However, it demonstrates weak performance again in the middle SoC range between 40% and 60%, not only because of the low percentage of accuracy but also the wide range of incorrectly allocated cluster numbers. Almost same discussion is valid for the results presented in other parts of Fig. 8 where different sets of inputs are used. The confusion matrix presented in Fig. 8(f) shows the best performance of the proposed classifier in which all the Thevenin parameters are used. Even in that case, the results are not perfect however, they are very promising. In Section 4, combination of coulomb-counting and the proposed classifier is presented in form of a hybrid system to achieve higher accuracy.

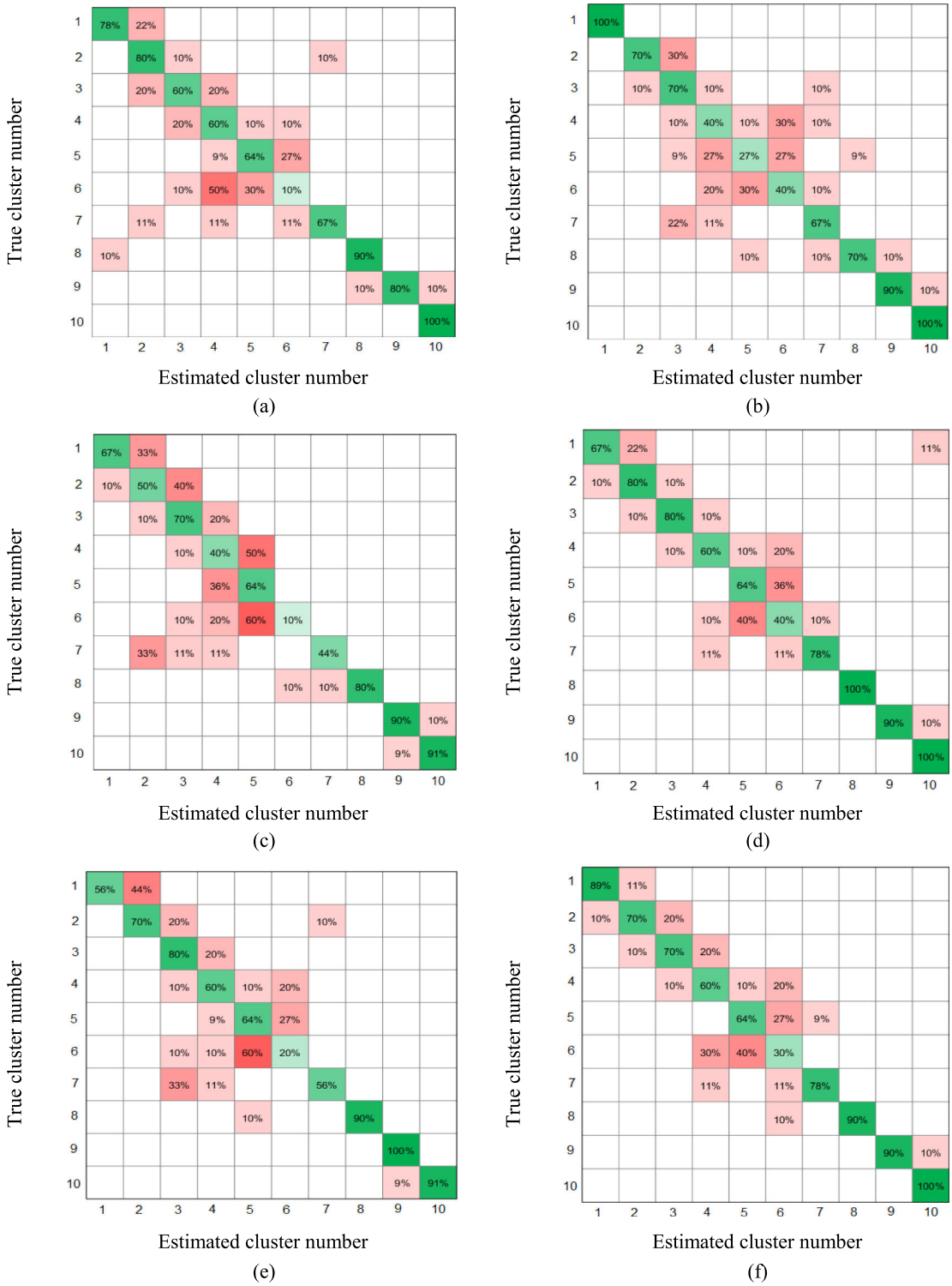

Fig. 8. Confusion matrices of SVM battery SoC classifier using different inputs: (a) V_{oc} and R_o, (b) V_{oc} and R_p, (c) V_{oc} and C_p, (d) R_o, R_p, and V_{oc}, (e) R_o, C_p, and V_{oc}, (f) V_{oc}, R_o, R_p, and C_p.

C. *Effect of Temperature*

In this section, the effect of temperature is investigated on both the identification and classification results. For this purpose, same algorithms are used however, they are applied on various test data sets which are obtained at different temperature levels. The MLTB test is repeated at 10 °C, 15 °C, 20 °C, 25 °C and 30 °C again from fully charged state until depletion. The thermal chamber that is presented in Section 2.2, is used to control the temperature. Since the discharge rates are not very high, we can assume that the cell's temperature is very close to the chamber temperature. To be sure about this, a thermal camera shown in

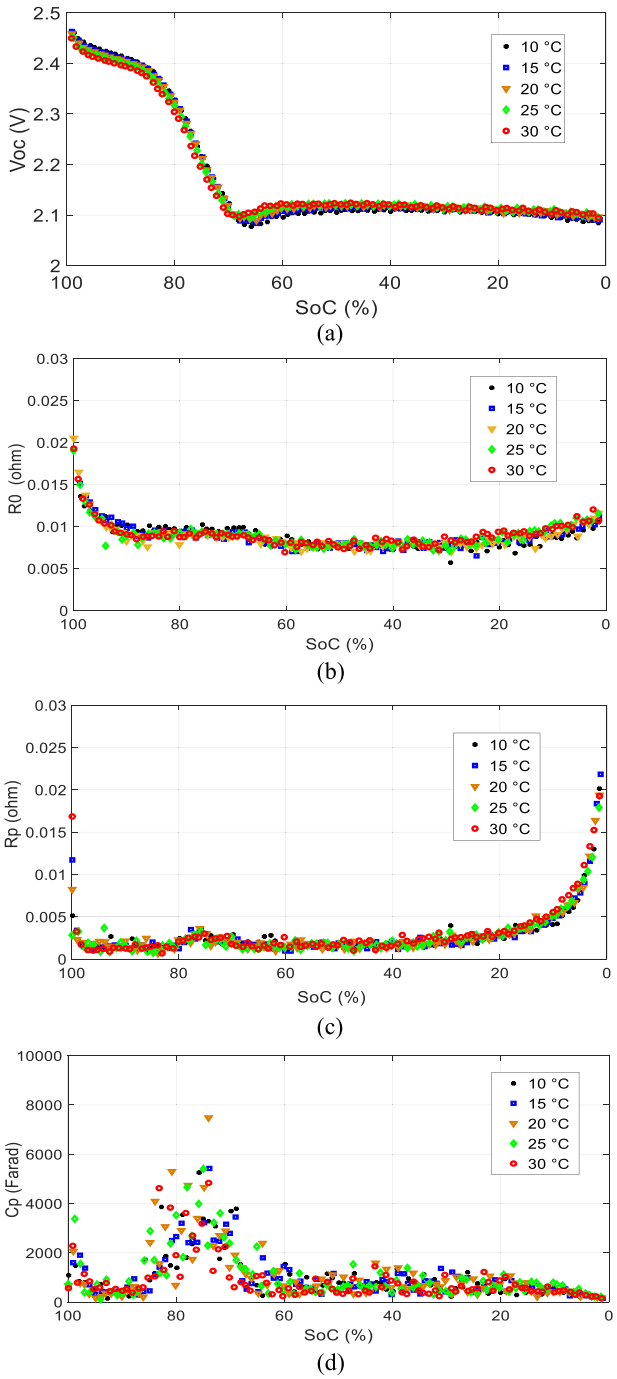

Fig. 9. The effect of temperature on the identification results: (a) V_{oc} , (b) R_o, (c) R_p, and (d) C_p.

Fig. 7is often used during the tests too. Fig. 9 illustrates the parameter identification results at different temperature levels. As shown in the figure, the algorithm is able to successfully identify the parameters under different conditions. Although the temperature slightly affects the Thevenin model's parameters, there is not a big difference in parameter values when switching between different temperatures. Robustness against the temperature is a very good feature of this new Li-S prototype cell comparing to the previous models presented in [49].

Similarly, the effect of the temperature is investigated on classification results. Table III contains the training and testing accuracy results of the SVM SoC classifier at different temperature levels. All results are obtained using the best input set that is V_{oc}, R_o, R_p and C_p as discussed in Section 3.2. The results demonstrate that the classification accuracy is not very much affected by temperature and the proposed algorithm works well in the whole range of temperature. In addition, Fig. 10 shows the confusion matrices of the best classifier (using four inputs) at different temperature levels. Although, the results are not exactly same at different temperatures, overall, the outcome is quite promising.

It should be mentioned that the implementation of this technique in real-time in a battery management system (BMS) will be as follows: first the range of operational temperature is determined at the design stage. Having the range of temperature, it should be discretized into smaller areas (for example every 5 °C as we did here). Then one separate classifier is trained for each temperature limit using the test data obtained at that particular temperature. Finally, in real-time application, temperature value is provided by a sensor and then the suitable classifier is selected.

IV. Li-S Cell SoC Estimation Using SVM Classifier and Coulomb-Counting: A Hybrid Method

In the previous sections, a classifier was designed to estimate Li-S cell SoC according to real-time ECN model parameterization. Although the classifier is able to give us the range of cell's SoC with a good approximation, it's improvement is possible in two directions: (i) the output of the classifier is a label that changes between 1 and 10; if this output is used directly, the SoC value can only be presented in form of fractions of 10% (i.e., 0%, 10%, 20%, and so on), However, we can improve it to generate a number that changes with resolution of 1% instead. (ii) the other direction of development is related to the fact that the output of the proposed classifier can jump from a number to another without considering the history of the predictions. This is due to the fact that the classifier only uses the identification outcomes at each time step. So, possible fluctuations in the identification results can easily lead to fluctuations in the SoC estimation.

In order to improve the proposed framework by addressing the above mentioned issues, a hybrid method is investigated in this section that works based on combination of two estimation techniques: coulomb-counting and SVM. The hybrid method uses benefits of both SVM and coulomb-counting while it gets rid of their limitations. According to the literature, coulomb-counting has disadvantageous such as accumulated error mainly due to measurement noise [12], [13]. In addition, it can only start working from a given initial SoC value which might not be available in real working condition. Another problem of using coulomb-counting is the change in battery capacity under different conditions which can cause an additional error.

To combine the classification technique and coulomb-counting, the first step is to convert the classifier's label to a value between 0 and 100 (i.e., SoC). In order to do this conversion,

TABLE III
SOC CLASSIFICATION RESULTS USING SVM AND DIFFERENT TEMPERATURES FOR $V_{oc}/R_o/R_p/C_p$ INPUTS

	Temperature values				
	10°C	15°C	20°C	25°C	30°C
Training accuracy	86%	88%	91%	90%	87%
Testing accuracy (hard clustering)	65%	82%	78%	73%	70%
Testing accuracy (soft clustering)	97%	93%	96%	93%	96%

the middle value of each cluster is considered as follows:

$$\begin{cases} \text{SoC of cluster 1 } (0-10\%) : 5\% \\ \text{SoC of cluster 2 } (10-20\%) : 15\% \\ \quad \ldots \\ \text{SoC of cluster 10 } (90-100\%) : 95\% \end{cases} \tag{21}$$

By this conversion, the classifier's output can be mixed with coulomb-counting method's SoC that also changes between 0 and 100. The next step is to combine the two estimations using a mathematical formulation such as follows:

$$SoC_H = \frac{\boldsymbol{W}1.\boldsymbol{SoC_{SVM}} + \boldsymbol{W}2.\boldsymbol{SoC_{coulomb-counting}}}{\boldsymbol{W}1 + \boldsymbol{W}2} \tag{22}$$

Where SoC_H is the hybrid SoC, SoC_{SVM} is the SoC coming from SVM and$SoC_{coulomb-counting}$ is the SoC from coulomb-counting. $W1$ and $W2$ are the fusion gains given to estimated values of SVM and coulomb-counting respectively. Using these gains, we can give different value to each estimator (not necessarily equal). Coulomb-counting algorithm starts from an initial guess value (i.e., considered to be 50% in this study) and it is updated at each iteration by integration of current (consumed Ah) in a short period of time until the next iteration. At each iteration, the algorithm is initialized from the previous value of SoC_H to eliminate the accumulated error. On the other hand, SVM does the estimation separately based on the identification results at each iteration. Finally, the outcomes of both methods are combined using the fusion gains as presented in (21).

The proposed hybrid method is simulated under different initial conditions as presented later in this section. In order to evaluate its performance, the 'theoretical' coulomb-counting is used as a benchmark. Such a benchmark is only available after finishing a test because it uses the real achievable capacity (not the nominal capacity). In this article, the benchmark is called 'true SoC', 'correct SoC' or 'reference SoC' in the following parts.

The advantage of SVM is that it can provide a better guess of the initial condition at the beginning. This can be controlled by changing the fusion gains, $W1$ and $W2$, accordingly. For example when $W1 > W2$, more trust is on SVM which leads to a quicker convergence however, after convergence it fluctuates more around the reference SoC. In the other case, when $W2 > W1$, more trust is on coulomb-counting which leads to a slower convergence however, after convergence it remains very close to the reference SoC. Fig. 11(a) and (b) illustrates the results of two cases in which W1 $= 0.3$, W2 $= 0.7$ and then W1 $= 0.7$, W2 $= 0.3$ respectively. As shown in Fig. 11(a), the real test starts from 100% SoC while the estimator starts from 50% because it doesn't know about the true SoC. The estimator then converges to the true SoC value gradually. The convergence rate is low in this case since more trust is on coulomb-counting (W2 $= 0.7$). In the other case presented in Fig. 11(b), more trust is on SVM (W1 $= 0.7$). In that case, the estimator converges quicker however, it fluctuates more around the reference SoC after convergence.

Regarding the results presented in Fig. 11 that demonstrate the importance of fusion gains on performance of the estimator, a question is raised: how can we get the best performance of the estimator by changing the fusion gains? In both aforementioned cases, the fusion gains were constant in the whole range of SoC. However, referring to the classification results presented in Section 3.2, the accuracy of SVM varies at different SoC values. Therefore, one solution to improve the estimator's performance is to change the fusion gains in real-time (adaptive gains). For example, giving more value to the SVM when the uncertainty in SoC_{SVM} is lower and vice versa. Let's look again at the results presented in Fig. 11(a) and (b); what can we do to have both advantages of quick convergence and less fluctuations after convergence. Constant gains cannot produce better results, but what will happen if we use a set of gains at the beginning and then switch to another one? In theory, when we fix the gains over the whole range of SoC, the hybrid technique has less flexibility to maximise the benefit from both SVM and coulomb-counting methods at the same time. However, when the fusion gains can change over the range of SoC, we can play with the numbers and find the best trade-off to achieve the best convergence rate at the beginning while having the best performance after the convergence as well.

Table IV presents the estimation results in different cases including the two aforementioned sets of constant gains and also new cases in which the fusion gains are variable. For results comparison, the average and maximum estimation errors after convergence, and the convergence rate (in form of number of iterations) are investigated. As presented in Table IV, case 1 is better than case 2 in terms of error values however, it suffers from slow convergence. On the other hand, case 2 outperforms case 1 in terms of convergence rate since it more relies on SVM. In case 3 for example, the gains of W1 $= 0.7$, W2 $= 0.3$ (i.e., SVM dominant) are same as case 2 at the beginning however, after initial iterations, the gains change to W1 $= 0.3$, W2 $= 0.7$ (i.e., coulomb-counting dominant). Case 3 has both advantages of case 1 and 2 using variable fusion gains. It converges quickly

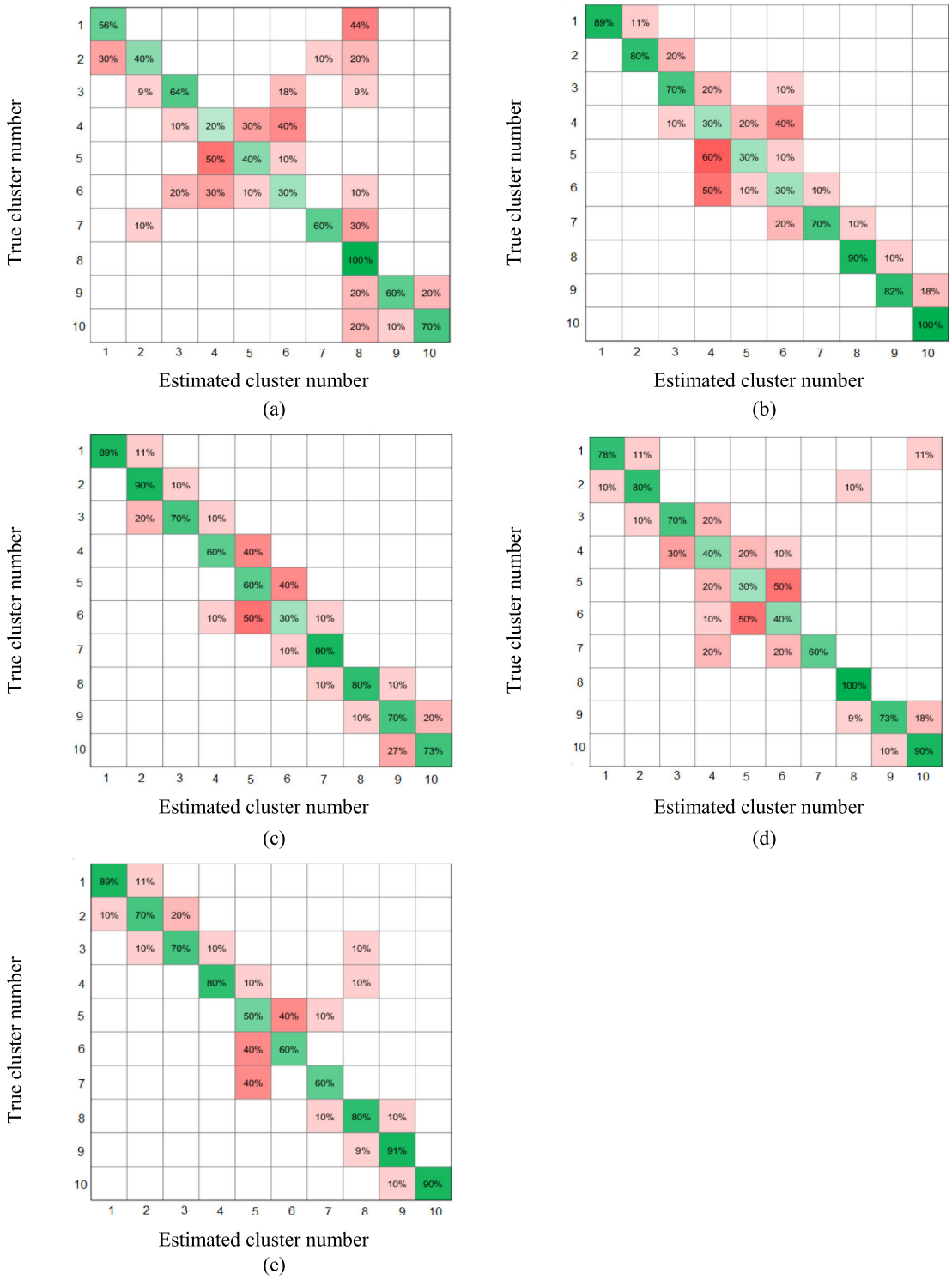

Fig. 10. Confusion matrices of SVM battery SoC classifier at different temperature: (a) 10 °C, (b) 15 °C, (c) 20 °C, (d) 25 °C, (e) 30 °C.

at the beginning using SVM and then controls the fluctuations by relying more on coulomb-counting. It should be noted that we cannot rely 100% on coulomb-counting even after convergence, since it can gradually deviate from the reference SoC. That is because of the accumulative noise effect and the nominal capacity that is used in its formulation. In the proposed hybrid technique with variable gains, SVM modifies any potential error in coulomb-counting gradually at each iteration.

In order to find the best ratio between the fusion gains, different configurations have been investigated as listed in Table IV (cases 3-7). According to the results, the best performance is achieved in case 5 where W1 = 0.9 and W2 = 0.1 at the

TABLE IV
Li-S CELL SOC ESTIMATION ACCURACY USING HYBRID METHOD WITH DIFFERENT FUSION GAINS (INITIAL SOC = 100%)

	Initial fusion gains	Fusion gain after convergence	Average error (%) after convergence	Maximum error (%) after convergence	Convergence rate (number of iterations)
Case 1	W1=0.3, W2=0.7 (constant)		1.04	4.03	8
Case 2	W1=0.7, W2=0.3 (constant)		2.03	4.45	4
Case 3	W1=0.7, W2=0.3	W1=0.3, W2=0.7	1.07	3.68	4
Case 4	W1=0.8, W2=0.2	W1=0.2, W2=0.8	0.75	2.63	4
Case 5	W1=0.9, W2=0.1	W1=0.1, W2=0.9	0.59	3.76	3
Case 6	W1=0.95, W2=0.05	W1=0.05, W2=0.95	0.99	3.36	3
Case 7	W1=1, W2=0	W1=0, W2=1	3.72	6.38	2

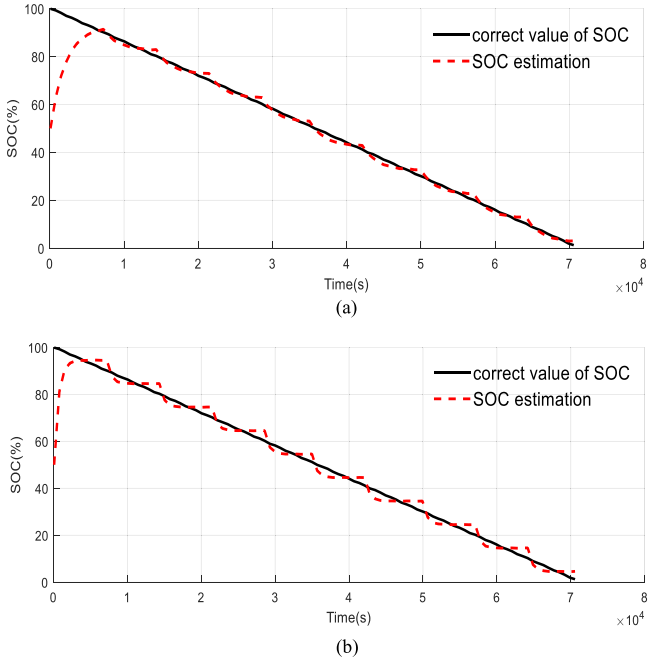

Fig. 11. True SoC vs. SoC estimation: (a) Fusion gains: W1 = 0.3, W2 = 0.7 (b) Fusion gains: W1 = 0.7, W2 = 0.3.

beginning and they change to W1 = 0.1 and W2 = 0.9 after convergence.

As a final analysis, different initial conditions are tested to evaluate the proposed technique under more realistic conditions. In a real application such as an EV, the BMS might start working from any initial condition. So, the SoC estimator should be able to converge to the true SoC value in a reasonable time. To investigate that, four case-studies are considered where only part of the test data is provided to the estimator (starting from unknown initial conditions). Fig. 12 shows the estimated SoC vs. true SoC under four initial conditions, 100%, 70%, 40% and 20%. According to the results, the proposed estimator is able to produce acceptable results in all four cases. This is a significant achievement particularly for Li-S battery that is more challenging than other types of battery in terms of SoC estimation [15].

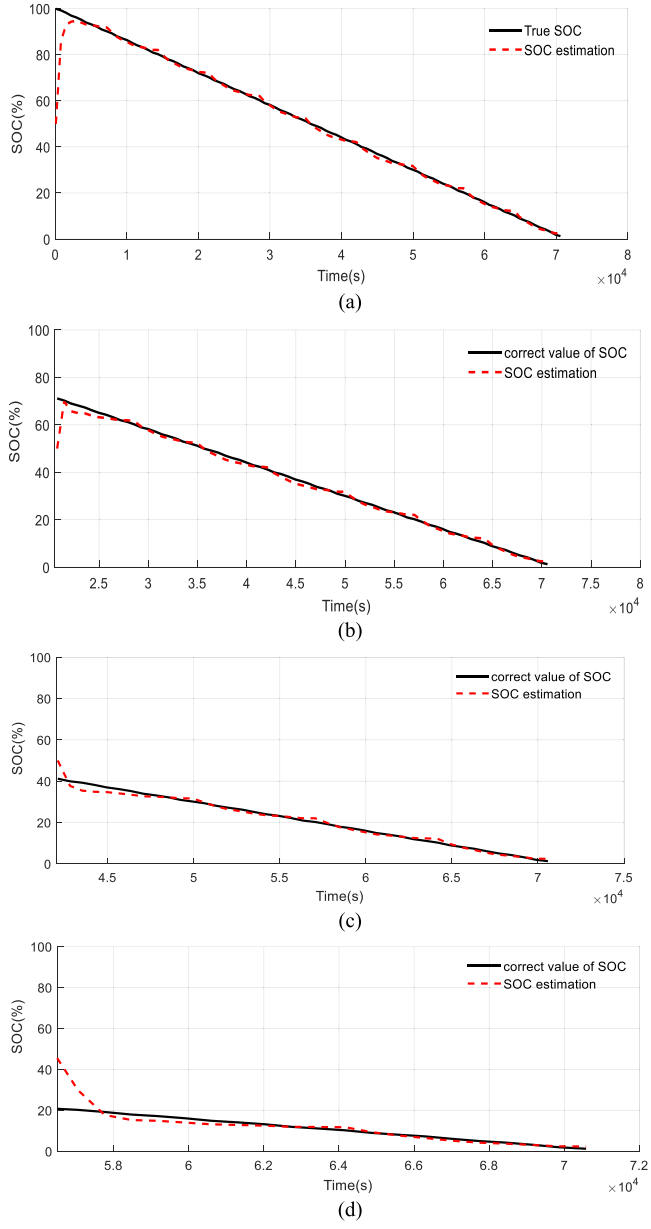

Fig. 12. True SoC vs. SoC estimation using variable fusion gains: (a) initial SoC = 100%, (b) initial SoC = 70%, (c) initial SoC = 40%, (d) initial SoC = 20%.

V. Conclusion

In this study, a new SoC estimation technique was developed for a new prototype Li-S cell. For this purpose, a number of experiments were conducted on individual cells under MLTB working condition and then an ECN model was parameterized using FFRLS identification algorithm. The proposed idea was to perform parameter identification in real-time and then use it in a classifier such as SVM to give an approximation of the cell's SoC. Although the proposed method requires offline training, its advantage is that it does not need data storage in real-time or either the initial SoC value. The classification results showed that Li-S cell SoC is less observable in the middle range (30%-70% SoC) that is in accordance to the previous published results in the literature. Against the complexities in Li-S cell SoC estimation, the proposed hybrid method has demonstrated promising results where coulomb-counting was combined with SVM and FFRLS. According to the results (which are validated by using experimental test data), the proposed hybrid method is able to estimate Li-S cell's SoC from any initial condition with maximum error of 2.63% and average error less than 1%.

As an extension of this study, the effect of ageing can be considered too. Because the parameters of the ECN model are influenced by cell aging, a modification factor should be added to the estimator to compensate the effect of ageing.

Acknowledgment

The authors thank OXIS Energy for their help and support.

The data used in this article is described in CORD at 10.17862/cranfield.rd.12011220; it is subject to an embargo, and will be available from 1 April 2031.

References

[1] A. F. Hofmann, D. N. Fronczek, and W. G. Bessler, "Mechanistic modeling of polysulfide shuttle and capacity loss in lithium-sulfur batteries," *J. Power Sources*, vol. 259, pp. 300–310, 2014.

[2] L. Lam and P. Bauer, "Practical capacity fading model for li-ion battery cells in electric vehicles," *IEEE Trans. Power Electron.*, vol. 28, no. 2, pp. 5910–5918, Dec. 2013.

[3] A. Fotouhi, D. J. Auger, K. Propp, and S. Longo, "Lithium-sulfur battery state-of-charge observability analysis and estimation," *IEEE Trans. Power Electron.*, vol. 33, no. 7, pp. 5847–5859, Jul. 2018.

[4] I. S. Kim, "Nonlinear state of charge estimator for hybrid electric vehicle battery," *IEEE Trans. Power Electron.*, vol. 23, no. 4, pp. 2027–2034, Jul. 2008.

[5] J. C. A. Antón, P. J. G. Nieto, F. J. de Cos Juez, F. S. Lasheras, C. B. Viejo, and N. R. Gutiérrez, "Battery state-of-charge estimator using the MARS technique," *IEEE Trans. Power Electron.*, vol. 28, no. 8, pp. 3798–3805, Aug. 2013.

[6] H. Chaoui and C. C. Ibe-Ekeocha, "State of charge and state of health estimation for lithium batteries using recurrent neural networks," *IEEE Trans. Veh. Technol.*, vol. 66, no. 10, pp. 8773–8783, Oct. 2017.

[7] J. C. A. Antón, P. J. G. Nieto, C. B. Viejo, and J. A. V. Vilán, "Support vector machines used to estimate the battery state of charge," *IEEE Trans. Power Electron.*, vol. 28, no. 12, pp. 5919–5926, Dec. 2013.

[8] M. U. Cuma and T. Koroglu, "A comprehensive review on estimation strategies used in hybrid and battery electric vehicles," *Renewable Sustain. Energy Rev.*, vol. 42, pp. 517–531, 2015.

[9] J. Li, J. K. Barillas, C. Guenther, and M. A. Danzer, "A comparative study of state of charge estimation algorithms for lifepo4 batteries used in electric vehicles," *J. Power Sources*, vol. 230, pp. 244–250, 2013.

[10] C. H. Cai, D. Du, and Z. Y. Liu, "Battery State-of-Charge (SOC) estimation using adaptive neuro-fuzzy inference system (ANFIS)," in *Proc. 12th IEEE Int. Conf. Fuzzy Syst.*, 2003, pp. 1068–1073.

[11] X. Hu, F. Feng, K. Liu, L. Zhang, J. Xie, and B. Liu, "State estimation for advanced battery management: Key challenges and future trends," *Renewable Sustain. Energy Rev.*, vol. 114, 2019, Art. no. 109334.

[12] B. Pattipati, C. Sankavaram, and K. Pattipati, "System identification and estimation framework for pivotal automotive battery management system characteristics," *IEEE Trans. Syst., Man, Cybern., Part C: Appl. Rev.*, vol. 41, pp. 869–884, Nov. 2011.

[13] K. Kutluay, Y. Cadirci, Y. S. Ozkazanc, and I. Cadirci, "A new online state-of-charge estimation and monitoring system for sealed lead-acid batteries in telecommunication power supplies," *IEEE Trans. Ind. Electron.*, vol. 52, pp. 1315–1327, Oct. 2005.

[14] J. Xu, C. C. Mi, B. Cao, J. Deng, Z. Chen, and S. Li, "The state of charge estimation of lithium-ion batteries based on a proportional-integral observer," *IEEE Trans. Veh. Technol.*, vol. 63, no. 4, May 2013.

[15] A. Fotouhi, D. J. Auger, K. Propp, and S. Longo, "Electric vehicle battery parameter identification and SOC observability analysis: NiMH and Li-S case studies," *IET Power Electron.*, vol. 10, no. 11, pp. 1289–1297, 2017.

[16] W. He, N. Williard, C. Chen, and M. Pecht, "State of charge estimation for electric vehicle batteries using unscented kalman filtering," *Microelectron. Rel.*, vol. 53, no. 6, pp. 840–847, 2013.

[17] G. L. Plett, "Extended kalman filtering for battery management systems of lipb-based HEV battery packs: Part 1. Background," *J. Power Sources*, vol. 134, pp. 252–261, 2004.

[18] G. L. Plett, "Sigma-point kalman filtering for battery management systems of lipb-Based HEV battery packs, part 2: Simultaneous state and parameter estimation," *J. Power Sources*, vol. 161, pp. 1369–1384, 2006.

[19] F. Sun, X. Hu, Y. Zou, and S. Li, "Adaptive unscented kalman filtering for state of charge estimation of a lithium-ion battery for electric vehicles," *Energy*, vol. 36, no. 5, pp. 3531–3540, 2011.

[20] L. Zhong, C. Zhang, Y. He, and Z. Chen, "A method for the estimation of the battery pack state of charge based on in-pack cells uniformity analysis," *Appl. Energy*, vol. 113, pp. 558–564, 2014.

[21] X. Liu, Z. Chen, C. Zhang, and J. Wu, "A novel temperature-compensated model for power Li-ion batteries with dual-particle-filter state of charge estimation," *Appl. Energy*, vol. 123, pp. 263–272, 2014.

[22] S. Schwunk, N. Armbruster, S. Straub, J. Kehl, and M. Vetter, "Particle filter for state of charge and state of health estimation for lithium–iron phosphate batteries," *J. Power Sources*, vol. 239, pp. 705–710, 2013.

[23] C. Zheng, Y. Fu, and C. C. Mi, "State of charge estimation of lithium-ion batteries in electric drive vehicles using extended kalman filtering," *IEEE Trans. Veh. Technol.*, vol. 62, no. 3, pp. 1020–1030, Mar. 2013.

[24] M. S. E. Din, M. F. Abdel-Hafez, and A. A. Hussein, "Enhancement in li-ion battery cell state-of-charge estimation under uncertain model statistics," *IEEE Trans. Veh. Technol.*, vol. 65, no. 6, pp. 4608–4618, Jun. 2016.

[25] H. Rahimi-Eichi, F. Baronti, and M. Y. Chow, "Online adaptive parameter identification and state-of-charge coestimation for lithium-polymer battery cells," *IEEE Trans. Ind. Electron.*, vol. 61, no. 4, pp. 2053–2061, Apr. 2014.

[26] A. Fotouhi, D. J. Auger, K. Propp, and S. Longo, "Accuracy versus simplicity in online battery model identification," *IEEE Trans. Syst., Man Cybern.: Syst.*, vol. 48, no. 2, pp. 195–206, Feb. 2018.

[27] C. H. Cai, D. Du, and Z. Y. Liu, "Battery state-of-charge (SOC) estimation using adaptive neuro-fuzzy inference system (ANFIS)," in *Proc. IEEE Int. Conf. Fuzzy Syst.*, 2003, pp. 1068–1073.

[28] M. F. Tsai, Y. Y. Peng, C. S. Tseng, and N. S. Li, "Modeling and estimation of state of charge for lithium-ion batteries using ANFIS architecture," in *Proc. IEEE Int. Symp. Ind. Electron.*, 2012, pp. 863–868.

[29] K. Propp, D. J. Auger, A. Fotouhi, S. Longo, and V. Knap, "Kalman-variant estimators for state of charge in lithium-sulfur batteries," *J. Power Sources*, vol. 343, pp. 254–267, 2017.

[30] K. Propp, D. J. Auger, A. Fotouhi, M. Marinescu, V. Knap, and S. Longo, "Improved state of charge estimation for lithium-sulfur batteries," *J. Energy Storage*, vol. 26, 2019, Art. no. 100943.

[31] V. Knap, D. Auger, K. Propp, A. Fotouhi, and D.- I. Stroe, "Concurrent real-time estimation of state of health and maximum available power in lithium-sulfur batteries," *Energies*, vol. 11, no. 8, 2018, Art. no. 2133.

[32] C. Paleologu, J. Benesty, and S. Ciochina, "A robust variable forgetting factor recursive least-squares algorithm for system identification," *IEEE Signal Process. Lett.*, vol. 15, pp. 597–600, 2008.

[33] W. K. Yung and K. F. Man, "Optimal selected forgetting factor for RLS estimation," *IFAC Proc.*, vol. 26, no. 2, pp. 331–334, 1993.

[34] M. H. Hayes, *Statistical Digital Signal Processing and Modeling*. New York, NY, USA: Wiley, 1996.

[35] C. Cortes and V. Vapnik, "Support-vector networks," *Mach. Learn.*, vol. 20, pp. 273–297, 1995.

[36] X. Li, D. Lord, Y. Zhang, and Y. Xie, "Predicting motor vehicle crashes using support vector machine models," *Accident Anal. Prev.*, vol. 40, pp. 1611–1618, 2008.
[37] T. Hansen and C. J. Wang, "Support vector based battery state of charge estimator," *J. Power Sources*, vol. 141, pp. 351–358, 2005.
[38] X. Wu, L. Mi, W. Tan, J. L. Qin, and M. N. Zhao, "State of charge (SOC) estimation of Ni-MH battery based on least square support vector machines," *Adv. Mater. Res.*, AMR.211-212.1204, 2011.
[39] J. C. Á. Antón, P. J. G. Nieto, F. J. de Cos Juez, F. S. Lasheras, M. G. Vega, and M. N. R. Gutiérrez, "Battery state-of-charge estimator using the SVM technique," *Appl. Math. Modelling*, vol. 37, no. 9, pp. 6244–6253, 2013.
[40] Z. Deng, L. Yang, Y. Cai, H. Deng, and L. Sun, "Online available capacity prediction and state of charge estimation based on advanced data-driven algorithms for lithium iron phosphate battery," *Energy*, vol. 112, 2016, Art. no. 469e480.
[41] J. C. A. Anton, P. J. G. Nieto, C. B. Viejo, and J. A. V. Vilan, "Support vector machines used to estimate the battery state of charge," *IEEE Trans. Power Electron.*, vol. 28, no. 12, pp. 5919–5926, Dec. 2013.
[42] J. N. Hu *et al.*, "State-of-charge estimation for battery management system using optimized support vector machine for regression," *J. Power Sources*, vol. 269, pp. 682–693, 2014.
[43] Q.-S. Shi, C.-H. Zhang, and N.-X. Cui, "Estimation of battery state-of-charge using ν-support vector regression algorithm," *Int. J. Automot. Technol.*, vol. 9, no. 6, pp. 759–764, 2008.
[44] OXIS Energy, "Our cell and battery technology advantages," OXIS Energy website, Accessed: Mar. 19, 2020. [Online]. Available: http://www.oxisenergy.com/technology/
[45] T. J. Barlow, S. Latham, I. S. McCrae, and P. G. Boulter, *A Reference Book of Driving Cycles for Use in the Measurement of Road Vehicle Emissions*. Wokingham: TRL Ltd, 2009, [Online]. Available: https://assets.publishing.service.gov.uk/government/uploads/system/uploads/attachment_data/file/4247/ppr-354.pdf
[46] Low Carbon Vehicle Partnership, "Testing & accreditation (LCEB certification)," LCVP website, 2018, Accessed: May 1, 2018. [Online]. Available: https://www.lowcvp.org.uk/initiatives/lceb/lceb-testing.htm
[47] A. Fotouhi, D. J. Auger, K. Propp, S. Longo, and M. Wild, "A review on electric vehicle battery modelling: From lithium-ion toward lithium-sulphur," *Renewable Sustain. Energy Rev.*, vol. 56, pp. 1008–1021, 2016.
[48] H. He, R. Xiong, and J. Fan, "Evaluation of lithium-ion battery equivalent circuit models for state of charge estimation by an experimental approach," *Energies*, vol. 4, pp. 582–598, 2011.
[49] A. Fotouhi *et al.*, "Lithium-sulfur cell equivalent circuit network model parameterization and sensitivity analysis," *IEEE Trans. Veh. Technol.*, vol. 66, no. 9, pp. 7711–7721, Sep. 2017.
[50] Z. M. Salameh, M. A. Casacca, and W. A. Lynch, "A mathematical model for lead-acid batteries," *IEEE Trans. Energy Convers.*, vol. 7, no. 1, pp. 93–98, Mar. 1992.
[51] I. Steinwart and A. Christmann, *Support Vector Machines*. New York, NY, USA: Springer, 2008.

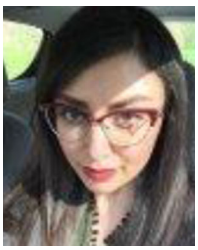

Neda Shateri received the M.Sc. degree in systems and control from Coventry University in 2018. She is currently working toward the Ph.D. degree in advanced vehicle engineering centre with Cranfield University. Her research interests include degradation modeling and state estimation of Lithium-Sulfur battery in real-world applications such as a vehicle powertrain system. She is particularly interested in investigation of the impacts of different temperature and c-rates on battery degradation. She has expertise in dynamical systems modeling and simulation, control and optimization.

Zhihao Shi was born in Jiangsu, China, in 1987. She received the master's degree in electrical engineering from the University of Nantes in 2011, and the Ph.D. degree from the University of Nantes in 2014. She is currently R&D Engineer with PSA Automobile in France. Her research interest includes state estimation of batteries for automotive industry.

Daniel J. Auger (Senior Member, IEEE) was born in Rainham, Kent, U.K., in 1977. He received the M.Eng. and Ph.D. degrees from the University of Cambridge in 2000 and 2005, respectively. From 2004 to 2008, he was a Senior Engineer with BAE Systems. From 2008 to 2013, he was a Senior Consultant with MathWorks. He was with Cranfield University's Advanced Vehicle Engineering Centre in 2013 and is currently Reader in electrification, automation and control. His battery-related research interests include hybrid energy storage systems, state estimation, and electrical/thermal modeling. He also has a general interest in applications of modeling and control to vehicle systems, including driving automation and ADAS systems. He is a Former Chair of the IEEE U.K. & Ireland Control Systems Society Chapter, an IET Fellow and a Chartered Engineer.

Abbas Fotouhi (Member, IEEE) received the Ph.D. degree in mechanical engineering from the Iran University of Science and Technology, Tehran, Iran, in 2011. He is currently a Lecturer in advanced vehicle engineering centre with Cranfield University. He has expertise in dynamical systems modeling, simulation, optimization, and control. He has also extensive practical and algorithmic experience of applying AI and Machine Learning techniques in engineering problems. His current research interests include electrified powertrain systems, energy storage technologies, and transportation systems. He is a fellow of the U.K. Higher Education Academy and fellow of the Faraday Institution in U.K.

2020-12-16

Lithium-sulfur cell state of charge estimation using a classification technique

Shateri, Neda

IEEE

Shateri N, Shi Z, Auger DJ, Fotouhi A. (2021) Lithium-sulfur cell state of charge estimation using a classification technique. IEEE Transactions on Vehicular Technology, Volume 70, Issue 1, January 2021, pp. 212-224

https://doi.org/ 10.1109/TVT.2020.3045213